Water-mass control on phytoplankton spatiotemporal variations in the northeastern East China Sea and the western Tsushima Strait revealed by lipid biomarkers

Rong Bi[1,2], Xi Chen[1], Jing Zhang[3*,1,2], Joji Ishizaka[4], Yanpei Zhuang[5], Haiyan Jin[5], Hailong Zhang[1], Meixun Zhao[1,2*]

[1] Key Laboratory of Marine Chemistry Theory and Technology (Ocean University of China), Ministry of Education, Qingdao 266100, China

[2] Laboratory for Marine Ecology and Environmental Science, Qingdao National Laboratory for Marine Science and Technology, Qingdao 266071, China

[3] Graduate School of Science and Engineering, University of Toyama, Gofuku 3190, Toyama 9308555, Japan

[4] Institute for Space-Earth Environmental Research (ISEE), Nagoya University, Nagoya, Aichi 464-8601, Japan

[5] Laboratory of Marine Ecosystem and Biogeochemistry, Second Institute of Oceanography, State Oceanic Administration, Hangzhou 310012, China

Corresponding author: Jing Zhang (jzhang@sci.u-toyama.ac.jp); Meixun Zhao (maxzhao@ouc.edu.cn, maxzhao04@yahoo.com)

Key Points:

- Phytoplankton biomass variations revealed by lipid biomarkers were controlled by water masses.
- The Changjiang Diluted Water was the main cause of high biomass in summer.
- Subsurface supply of nutrients was likely the main control on biomass variations in the open ocean water in autumn.

This article has been accepted for publication and undergone full peer review but has not been through the copyediting, typesetting, pagination and proofreading process which may lead to differences between this version and the Version of Record. Please cite this article as doi: 10.1002/2017JG004340

Abstract

Continental margin ecosystems in the western North Pacific Ocean are subject to strong climate forcing and anthropogenic impacts. To evaluate mechanisms controlling phytoplankton biomass and community structure variations in marginal sea-open ocean boundary regions, brassicasterol, dinosterol and C_{37} alkenones were measured in suspended particles in summer and autumn from 2012 to 2013 in the northeastern East China Sea and the western Tsushima Strait (NEECS-WTS). In summer, the concentrations of brassicasterol (40 - 1535 ng L^{-1}) and dinosterol (4.2 - 94 ng L^{-1}) were higher in the southwest of Cheju Island, while C_{37} alkenones (0 - 30 ng L^{-1}) were higher in the south of Cheju Island. In autumn, brassicasterol (12 - 106 ng L^{-1}), dinosterol (2.4 - 21 ng L^{-1}) and C_{37} alkenones (0.7 – 7.0 ng L^{-1}) were higher in the southwest of Cheju Island and the WTS, and higher C_{37} alkenones also occurred in the Okinawa Trough. Correlation analysis of biomarkers and environmental conditions (temperature, salinity and inorganic nutrient concentrations) clearly demonstrated that phytoplankton biomass and community structure variations can be well elucidated by water masses as indexed by temperature and salinity. High nutrients from the Changjiang River were the main cause of high biomass in summer, while nutrients from subsurface water were likely the key factor regulating phytoplankton biomass in open ocean water stations in autumn. This study indicates that mechanisms controlling phytoplankton biomass in marginal sea-open ocean boundary regions should be classified by various water masses with different nutrient concentrations, instead of by geography.

Key words

Phytoplankton biomass; Community structure; Biomarkers; Water masses; East China Sea; Tsushima Strait

1 Introduction

Margin seas of the western North Pacific Ocean are important regions to study the changing land-ocean interaction zone, due to the strong and complex influence of climate forcing and anthropogenic activities in this area (Liu et al., 2014). Such significant changes at the land-ocean boundaries have shown strong feedback into the global biogeochemical system (Chen et al., 2004; Chen & Borges, 2009).

The northeastern East China Sea and the western Tsushima Strait (NEECS-WTS) span between China, Korea and Japan, located at the shelf edge where the hydrography is strongly affected by the western boundary current, the Kuroshio. Thus, circulation systems and water masses in the NEECS-WTS are complex and characterized by the interaction of shelf water and the Kuroshio (Bai & Zhang, 2009; Liu et al., 2010). Five water masses exist throughout the year in the East China Sea (ECS) and adjacent areas: the Kuroshio Surface Water (KSW), the Kuroshio Intermediate Water, the East China Sea Surface Water (ECSSW), the Continental Coastal Water (CCW) and the Yellow Sea Surface Water, with the CCW, ECSSW and KSW showing strong seasonal variations in extent and temperature-salinity (*T*-*S*) properties (Qi et al., 2014). As a result, phytoplankton productivity in this area are affected by shelf and open ocean interactions, showing a broad pattern of high productivity in the shelf waters in summer and low productivity in the Kuroshio waters throughout the year (Gong et al., 2003; Kim et al., 2009; Liu et al., 2010). Also, phytoplankton distribution is dominated by water masses, with high abundances of diatoms and coccolithophores observed in the shelf and oceanic waters, respectively (Furuya et al. 1996; Kang et al., 2016). Recently, the Kuroshio has become weaker and warmer (Wang et al., 2016), and the concentration of chlorophyll-*a* (Chl-*a*) is also declining as the main stream of the Kuroshio is getting warmer in the western North Pacific (Aoyama et al., 2008). While NEECS-WTS is perfectly situated to systematically evaluate the roles of the shelf *versus* the open ocean water masses on biogeochemistry and ecology, there is insufficient data from direct observations to illustrate the spatiotemporal distribution of phytoplankton primary productivity and community structure, due to the special location of the NEECS-WTS (including exclusive economic zones) with very limited research ship access.

Lipid biomarkers have provided a powerful approach to study past and present Earth ecosystems based on their unique qualities (Bianchi and Canuel 2011). Lipid biomarkers can provide source specific information about ecosystem changes and they have been used for the paleo-reconstruction of phytoplankton productivity and community structure in both shelf sea and open ocean environments (Schubert et al., 1998; Xing et al., 2016; Zhao et al., 2006). Also in modern ecosystems, lipid biomarkers as a semi-quantitative approach have been used to reflect phytoplankton productivity (or biomass) and community composition (Hernandez et al., 2008; Li et al., 2014; Wu et al., 2016).

Previous studies on lipid biomarkers in the surface waters often focused on biomarker abundance and distributions in high-productivity periods such as during algal blooms (Hernandez et al., 2008) and in spring and summer (Wu et al., 2016). However, the patterns and mechanisms of phytoplankton biomass and community variations may differ seasonally. For example, mean values of phytoplankton abundance in the entire continental shelf area of the ECS in autumn were around 7 to 119 times higher than those in other three seasons of 2009-2011, with stratified water and medium nutrients (depth-integrated values: NO_3-N: 2.8-6.7 μmol L^{-1}; PO_4-P: 0.1-0.2 μmol L^{-1}; SiO_3-Si: 6.2-8.5 μmol L^{-1}) playing significant roles in regulating phytoplankton community structure in spring and summer, and turbulent water and high nutrients (NO_3-N: 7.3-8.7 μmol L^{-1}; PO_4-P: 0.4 μmol L^{-1}; SiO_3-Si: 9.9-14.1 μmol L^{-1}) as the main factors in autumn and winter (Guo et al., 2014). Also in the NEECS-WTS, high phytoplankton biomass in surface water in spring is supported by high nutrient concentrations from vertical mixing of water in winter, which has been revealed by spring biomarker distributions in the ECS in previous studies (e.g., Wu et al., 2016). However, in summer and autumn factors controlling nutrient concentrations are frequently not simple but are supported by the mixing of various water masses in the NEECS-WTS. The Changjiang Diluted Water (CDW) is one of the important nutrient sources even to the mid- and outer shelf in summer but the influence of the Kuroshio is more prominent in autumn (Kim et al., 2009; Zou et al., 1999). Therefore, biomarker studies in summer and autumn in the NEECS-WTS can be useful to disentangle the complexity of water mass-controlled phytoplankton biomass and community structure variations.

In this study, we applied a lipid biomarker approach to reveal the variations and controlling factors of phytoplankton biomass and community structure in the NEECS-WTS in summer and autumn of 2012-2013. Brassicasterol (24-methylcholesta-5,22E-dien-3β-ol), dinosterol (4α,23,24-trimethyl-5α-cholest-22-en-3β-ol) and C_{37} alkenones were measured from the surface suspended particles in the NEECS-WTS. The concentrations of brassicasterol, dinosterol and C_{37} alkenones can to some extent reflect the biomass of diatoms, dinoflagellates and haptophytes in the euphotic layer, respectively, and the sum of the three lipid biomarkers (∑PB) can be used as a total biomass proxy (Schubert et al., 1998; Wu et al., 2016; Xing et al., 2011). We also calculated the ratios of individual lipid biomarker and ∑PB as proxies of the proportion of each phytoplankton group biomass, and reported the distribution of temperature, salinity, Chl-*a*, and nutrients including dissolved inorganic nitrogen (DIN; NO_3-N and NO_2-N), dissolved inorganic phosphorus (DIP; PO_4-P) and silicate (Si; SiO_3-Si). In one of our previous studies, we focused on estuary-shelf sea interactions by measuring lipid biomarkers in suspended particles from the spring and summer in the ECS and the Southern Yellow Sea (SYS), which are located on the largest continental shelf of the western North Pacific Ocean (Wu et al., 2016). In the present study, we focus on marginal sea-open ocean interactions by conducting cruises in summer and autumn when the water masses are extremely complex. Thus, the aims of this study include: (i) to investigate the spatiotemporal distribution of phytoplankton lipid biomarkers in the NEECS-WTS in summer and autumn, and (ii) to understand the mechanisms (the shelf *versus* the open ocean water masses) controlling phytoplankton distribution patterns in the NEECS-WTS.

2 Oceanographic setting

The study area is located in the south of Cheju Island (N 27.5°-35°, E 124.5°-130°) and covers the NEECS-WTS and the northern Okinawa Trough (OT) (Fig. 1). Water depth in the study area ranges from 48 m in the Southern Yellow Sea to 1676 m in the northern OT, including mid- and outer shelf, and continental and island slope and trough. The CDW flows from the Changjiang River Estuary to the ECS outer shelf (Fig. 1 a and b), with a large run-off of the Changjiang River in summer (~50,000 m^3 s^{-1} at Station Datong) and a lower one in

winter (< 15,000 m^3 s^{-1} at Station Datong) (Yuan, 2015). The northward Kuroshio Current (KC) transports warm, hypohaline and oligotrophic water in the surface layer year around (Bian et al., 2013). Due to the strong southward wind in winter, the northward Taiwan Warm Current (TWC) is weaker in winter than in summer. The East China Sea Coastal Current in summer merges with the TWC and flows northeastward, while it flows southward in winter. The Tsushima Current originates from the KC and it flows through the Tsushima Strait in the surface layer year around.

3 Materials and Methods

3.1 Sample collection

Field observations and sampling were carried out on three summer cruises (8 - 18 July 2012, 30 June - 9 July 2013 and 13 July - 2 August 2013) and one autumn cruise (23 September - 2 October 2012) (Fig. 1 c and d). Surface water (0-5 m) temperature and salinity (using the Practical Salinity Scale) were measured in situ using a pre-calibrated conductivity-temperature-depth system CTD (SBE 9 plus, Sea-Bird Electronics *Inc.*, USA), and Chl-*a* was analyzed in situ using a chlorophyll fluorometer (Seapoint Sensors, *Inc*., United States). Lipid biomarker samples were collected from surface seawater at 51 stations in summer and 15 stations in autumn, obtained by filtration (water volume: 60-280 L) on Whatman GF/F filters (150 mm diameter) and stored at -20° C until analysis. Samples for DIN, DIP and Si analysis were taken at 36 stations in summer and 15 stations in autumn, with the seawater samples filtered through cellulose acetate membranes (pore size: 0.45μm).

3.2 Biomarker and nutrient analysis

Brassicaterol, dinosterol and C_{37} alkenones were measured after the procedure of Zhao et al. (2000). Lipid biomarker samples were first freeze-dried prior to further pre-treatment. The samples were extracted using the mixture of dichloromethane and MeOH (3:1, v/v), with the internal standard C_{19} *n*-alkanol added for quantification. Subsequently, the separation of apolar and polar fractions was carried out using silica gel chromatography (Qingdao Haiyang, 100-200 mesh, activated at 70 ℃ for 12h; app. 2 ml in *n*-hexane). The polar lipid fraction

contained sterols and C_{37} alkenones, and eluted with 22 ml dichloromethane/methanol (95:5, v/v). After elution, the polar fraction was silyated with 80 μl BSTFA (*N*, *O*-bis(trimethylsilyl)-trifluoroacetamide; 70 ℃, 1h). Lipid biomarker identification was performed on a gas chromatograph (Agilent 7890B GC; 30 m HP-5MS Ultra Inert capillary column, 0.25 mm i.d., 0.25 μm film thickness) connected to an Agilent 5977B mass selective detector (MSD, 70 eV constant ionization potential, ion source temperature 230 ℃). For biomarker quantification, the samples were analyzed by gas chromatography (Agilent 6890N GC-FID; 50 m HP-1 capillary column, 0.32 mm i.d., 0.17 μm film thickness). The GC oven temperature program started from 80 ℃ (holding for 1 min) and then increased to 200 ℃ at 25 ℃ min^{-1}, followed by 4 ℃ min^{-1} to 250 ℃, 1.8 ℃ min^{-1} to 300 ℃ (holding for 12 min), and finally holding at 300 ℃ for 5 min. Lipid biomarker contents were calculated according to the ratios of their GC peak integrations to that of the internal standard C_{19} *n*-alkanol.

Nutrient determination followed the procedure of Grasshoff et al. (1999) and the Specification for Oceanographic Survey (State Bureau of Quality and Technical Supervision, 2007). For the samples collected during the cruise of July 13 to August 2 of 2013, nitrite, phosphate and ammonia were detected immediately on board using 7230G Spectrophotometer, while samples for nitrate and silicate analysis were preserved with $HgCl_2$ immediately at -20° C and measured using a Continuous Flow Analyzer (Skalar San++, Skalar Analytical B.V., Netherlands). The samples collected in other cruises were first stored in a freezer and measured using a TRACCS 2000 autoanalyzer (Bran+Luebbe, Germany) after the cruises.

3.3 Data analysis

We used Spearman's rank correlation analysis to test the relationship between lipid biomarker concentrations (and lipid biomarker ratios) and temperature (and salinity and nutrients). The same analysis was done to test the relationship between ∑PB and Chl-*a*. Spearman's rank correlation analysis was conducted using SPSS 19.0 (IBM SPSS software), with significant level set to $p < 0.05$.

4 Results

Two high-biomass areas were established according to their biomarker concentrations (Fig. 1 c and d; Fig. 3). Area I (the southwest of Cheju Island) was identified due to its high concentrations of brassicasterol and ∑PB in summer and autumn. Mean values of brassicasterol and ∑PB in Area I were about three times higher than those of the whole study area (Table S1). Area II (the southwestern part of Tsushima Strait) was identified due to its high concentrations of brassicasterol, dinosterol and ∑PB in autumn. Mean values of brassicasterol, dinosterol and ∑PB in autumn in Area II were around two times higher than those of the whole study area.

4.1 Temperature, salinity and nutrient concentrations

Surface temperature ranged from 22.9 to 29.7° C (mean value: 27.5° C) in summer (Fig. 2 a; Table S1) and from 22.0 to 27.8° C (mean value: 24.9° C) in autumn (Fig. 2 f). The salinity ranged from 28.7 to 34.2 (mean value: 31.8) in summer (Fig. 2 b) and from 30.2 to 34.2 PSU (mean value: 32.9) in autumn (Fig. 2 g). In both seasons, temperature and salinity increased from the north to the south, showing lower values in Area I or in the north of Area I. Especially for salinity in summer, the mean value outside Area I (32.5) was 10% higher than that in Area I (29.6).

The concentrations of surface DIN, DIP and Si in summer varied from 0 to 4.1 μmol L^{-1} (mean value: 0.9 μmol L^{-1}), 0.02 to 0.2 μmol L^{-1} (mean value: 0.1 μmol L^{-1}), and 1 to 6.8 μmol L^{-1} (mean value: 3.2 μmol L^{-1}), respectively (Fig. 2 c-e). The mean value of DIN in Area I (2.0 μmol L^{-1}) was five times higher than that outside of Area I (0.4 μmol L^{-1}) (Fig. 2 c). The mean value of DIP in Area I (0.1 μmol L^{-1}) was 1.4 times higher than that outside of Area I (0.1 μmol L^{-1}) and it decreased from the west to the east in the study area (Fig. 2 d). The mean value of Si in Area I (3.7 μmol L^{-1}) was 1.3 times higher than that outside of Area I (2.9 μmol L^{-1}) and it decreased from the north to the south and the east (Fig. 2 e). In autumn, DIN (0.02 - 4.3 μmol L^{-1}; mean value: 0.7 μmol L^{-1}), DIP (0 - 0.4 μmol L^{-1}; mean value: 0.1 μmol L^{-1}) and Si (1.1 - 16.0 μmol L^{-1}; mean value: 4.0 μmol L^{-1}) had a similar distribution pattern, showing around two times higher in Area I than those outside of Area I (Fig. 2 h-j).

Mean values of temperature, salinity and each nutrient parameter were similar between summer and autumn, although the maximum values of DIP and Si in autumn were around two times higher than those in summer (Table S1; Fig. 2 d, e, i and j). The mean value of DIN concentration in summer was 1.2 times higher than that in autumn, while Si in autumn was 1.3 times higher than that in summer. Mean value of DIP was the same between the two seasons.

4.2 Lipid biomarkers and Chl-*a* in surface suspended particles

In summer, the concentration of brassicasterol ranged from 40.3 to 1535 ng L^{-1} (mean value: 274 ng L^{-1}), showing high values in Area I (424 - 1535 ng L^{-1}; mean value: 859 ng L^{-1}) (Fig. 3 a; Table S1). Dinosterol concentrations ranged from 4.2 to 94.3 ng L^{-1} (mean value: 33.7 ng L^{-1}), with high values in Area I (41.1 - 94.3 ng L^{-1}; mean value: 68.5 ng L^{-1}) and south of Area I (Fig. 3 b). C_{37} alkenones ranged from 0 to 30.2 ng L^{-1} (mean value: 4.5 ng L^{-1}), with high values occurred east of Area I and at two stations in the southern part of study area (Fig. 3 c). For ∑PB (52.6 - 1603 ng L^{-1}; mean value: 312 ng L^{-1}), high values occurred in Area I (477 - 1603 ng L^{-1}; mean value: 929 ng L^{-1}), resembling the distribution of brassicasterol (Fig. 3 d). Similarly, Chl-*a* (0.03 - 2.4 μg L^{-1}; mean value: 0.4 μg L^{-1}) also showed high values in Area I (0.2 - 2.4 μg L^{-1}; mean value: 0.9 μg L^{-1}) (Fig. 3 e).

In autumn, brassicasterol concentrations ranged from 12.1 to 106 ng L^{-1} (mean value: 54.3 ng L^{-1}), decreasing from the north to the south and showing high values in Area I (37.9 - 106 ng L^{-1}; mean value: 65.4 ng L^{-1}) and Area II (69.5 - 102 ng L^{-1}; mean value: 85.6 ng L^{-1}) (Fig. 3 f; Table S1). A similar distribution pattern was observed for dinosterol (2.4 - 20.5 ng L^{-1}; mean value: 8.8 ng L^{-1}), showing high values in Area I (4.3 - 14.7 ng L^{-1}; mean value: 8.9 ng L^{-1}) and Area II (12.3 – 20.5 ng L^{-1}; mean value: 16.4 ng L^{-1}) (Fig. 3 g). C_{37} alkenones (0.7 - 7.0 ng L^{-1}; mean value: 3.5 ng L^{-1}) had a broadly similar distribution pattern with brassicasterol and dinosterol, showing high values in Area I (1.4 - 7.0 ng L^{-1}; mean value: 3.7 ng L^{-1}) and Area II (4.2 - 7.0 ng L^{-1}; mean value: 5.6 ng L^{-1}), and at one station in the southern study area (3.5 ng L^{-1}) (Fig. 3 h). ∑PB (15.2 - 127 ng L^{-1}; mean value: 66.6 ng L^{-1}) exhibited a similar distribution pattern with brassicasterol and dinosterol, with high values in Areas I (48.3 -127 ng L^{-1}; mean value: 78.0 ng L^{-1}) and II (88.8 - 126 ng L^{-1}; mean value: 108

ng L^{-1}) (Fig. 3 i). Similar to ∑PB, Chl-*a* (0.2 to 3.0 μg L^{-1}; mean value: 1.0 μg L^{-1}) had high values in Areas I (0.5 - 3.0 μg L^{-1}; mean value: 1.7 μg L^{-1}) and II (1.073-1.077 μg L^{-1}; mean value: 1.075 μg L^{-1}) (Fig. 3 j).

Mean values of lipid biomarker concentrations in summer were higher than those in autumn, with values 5.3 times higher for ∑PB, 5.1 times higher for brassicasterol, 4.0 times higher for dinosterol and 1.4 times higher for C_{37} alkenones (Fig. 3 a-c and f-h; Table S1), while Chl-*a* in autumn was 2.8 times higher than that in summer (Fig. 3 e and j). For brassicasterol and dinosterol, high-value areas were located in Area I in summer, but in Area II and in the northeastern part of Area I in autumn. For C_{37} alkenones, high-value areas were located east of Area I in summer, but in Area II and in the northeastern part of Area I in autumn.

4.3 Individual lipid biomarker proportion (% of ∑PB) in surface suspended particles

In summer, brassicasterol/∑PB (B/∑PB) ranged from 45% to 96% (mean value: 81%), with high values in the northern part of the study area, especially in Area I (Fig. 4 a; Table S1). In contrast, high values for dinosterol/∑PB (D/∑PB) (4.3% to 50%; mean value: 15%) occurred in the southern part of the study area (Fig. 4 b). C_{37} alkenones/∑PB (A/∑PB) ranged from 0 to 21% (mean value: 3.6%), with one high-value area in the east of Area I and some high values at a few stations in the southern part of the study area (Fig. 4 c).

In autumn, B/∑PB ranged from 70% to 87% (mean value: 81%), with high values in Area I and the southeast of Area I (Fig. 4 e). In contrast, D/∑PB (8.7% to 17%; mean value: 13%) was high outside of Area I in the northeastern and southwestern part of the study area (Fig. 4 f). A/∑PB ranged from 1.1% to 14% (mean value: 6.0%), with high values in the southern part of study area, followed by some high values in the east of Area I (Fig. 4 g).

Spatial gradients of B/∑PB and D/∑PB in summer was much larger than that in autumn (Fig. 4 a, b, e and f). For B/∑PB, the maximum value in summer (located in Area I) was two times higher than the lowest one (located southeast of Area I), while in autumn the maximum value (located in Area I) was 1.3 times higher than the lowest one (located in the southern part of study area). For D/∑PB, the maximum value in summer (located southeast of Area I)

was 11 times higher than the lowest one (located in Area I), while in autumn the maximum value (located in the southern part of study area) was only two times higher than the lowest one (located in Area I). For A/∑PB, the maximum value in summer (21%) was located east of Area I, while C_{37} alkenones could not be detected at some stations in Area I, while in autumn the maximum value (located in the southern part of study area) was 12 times higher than the lowest one (located east of Area I).

4.4 Correlation analysis: biomarkers vs. temperature, salinity and nutrients

In summer, ∑PB showed significant positive correlations with Chl-*a* (Spearman's correlation coefficient $r = 0.716$; $p < 0.001$). Brassicasterol, dinosterol, and ∑PB correlated positively with DIN (and DIP, DIN:DIP and DIN:Si) ($p \leqslant 0.039$) and negatively with salinity ($p \leqslant 0.001$) (Table 1). Similarly, B/∑PB correlated positively with DIN, DIN:DIP and DIN:Si ($p \leqslant 0.014$) and negatively with salinity ($p \leqslant 0.001$). In contrast, C_{37} alkenones, D/∑PB, and A/∑PB correlated negatively with nutrients (DIN, DIN:DIP and DIN:Si) ($p \leqslant 0.043$) and positively with salinity ($p \leqslant 0.014$). D/∑PB also correlated positively with temperature, and dinosterol correlated negatively with Si:DIP ($p \leqslant 0.040$).

In autumn, ∑PB and Chl-*a* showed significant positive correlations ($r = 0.556$; $p = 0.039$), while brassicasterol, dinosterol, and ∑PB correlated negatively with Si:DIP in the whole study area ($p \leqslant 0.021$) (Table 2).

5. Discussion

Our study reveals highly variable concentrations of three lipid biomarkers in the NEECS-WTS in summer and autumn. The results show that distribution patterns of ∑PB and Chl-*a* were broadly similar in the whole study area, while the relationship between lipid biomarkers and environmental factors (temperature, salinity and nutrient concentrations) varied seasonally and differed between lipid biomarkers. Over the entire study area, mean values of temperature, salinity and nutrient concentrations in summer were similar to those in autumn (around 1 to 1.5 times difference), but mean values of lipid biomarker concentrations in summer were 1.4 to 5 times higher than those in autumn. However, in certain areas such as

Area II we observed higher concentrations of lipid biomarkers in autumn than those in summer. We thus discuss the use of lipid biomarkers as proxies of phytoplankton biomass and community structure, and water-mass related mechanisms controlling phytoplankton biomass and community structure variations in the NEECS-WTS in the following sections.

5.1 Lipid biomarkers reflect phytoplankton biomass and community structure

Lipid biomarkers in surface suspended particles can reflect phytoplankton biomass, as revealed by similar distribution patterns between lipid biomarkers and Chl-*a* and/or phytoplankton cell counting in previous studies (Dong et al., 2012; Sicre et al., 1994; Wu et al., 2016). In our study, we also observed a broadly similar distribution between ∑PB and Chl-*a*, i.e., high values in Area I in summer and in Areas I and II in autumn. Therefore, the similar distribution pattern and highly significant positive correlations between ∑PB and Chl-*a* in our study indicate that phytoplankton lipid biomarkers can be useful proxies for phytoplankton biomass and thus provide a means to examine the variation of phytoplankton biomass in the NEECS-WTS.

However, differences between the distributions of lipid biomarkers and Chl-*a* were also observed in our study. For example, the highest values of ∑PB and Chl-*a* were observed in the eastern part of Area I and the western part of Area I, respectively (Fig. 3 d, e, i and j), and the mean values of ∑PB were higher in summer and those of Chl-*a* were higher in autumn (Table S1). Similarly, conflicting conclusions derived from lipid and pigment biomarkers were also found in previous studies (Ras et al., 2008; Tolosa et al., 2008; Wu et al., 2016). Different distributions between ∑PB and Chl-*a* in our study can be explained by taxonomic specificity of lipid biomarkers and the influences of environmental factors on the quantitative relationship between photosynthetic pigment Chl-*a* and lipid biomarkers (Wu et al., 2016). In addition to diatoms and dinoflagellates, autotrophic picophytoplankton such as *Prochlorococcus* and *Synechococcus* are also important phytoplankton groups in the offshore area of the ECS (Furuya et al., 2003; Guo et al., 2014; Jiao et al., 2005), which may contribute largely to total Chl-*a*, especially in summer (Liu et al., 2016). Additional factors such as different resolutions between summer and autumn cruises, with a high-resolution survey in summer (51 stations) and a lower one in autumn (15 stations), may also cause

inconsistent information revealed by pigment and lipid proxies. While Chl-*a* has been widely used as a proxy for the total biomass of primary producers, ∑PB could also show more information on specific subsets of phytoplankton.

Indeed, the normalized concentrations of lipid biomarkers in the suspended particles can be useful proxies for phytoplankton community structure as revealed by similar distribution patterns between lipid biomarkers and corresponding pigments and/or microscopic counting in different study areas such as in the northeastern Atlantic (Mejanelle et al., 1995) and in the ECS and SYS (Wu et al., 2016). Our study shows the order of brassicasterol > dinosterol > C_{37} alkenones (concentrations; both maximum and mean values) and B/∑PB (45%-96%) > D/∑PB (4.3%-50%) > A/∑PB (0-20.77%) in the NEECS-WTS in summer and autumn. The relatively high values of B/∑PB suggest the dominance of diatoms, consistent with the results in the NEECS-WTS and adjacent areas in previous studies using small subunit ribosomal RNA pyrosequencing (Boopathi et al., 2015) and microscopic counting (Guo et al, 2011; Jang et al., 2013). For example, Guo et al. (2011) studied phytoplankton assemblages in the PN section of the ECS in summer by the Utermöhl method, showing that *Bacteriastrum comosum* and *Chaetoceros decipiens* were the dominant diatom species in offshore areas influenced by the Kuroshio intrusion. Hence, the consistent results between our study and previous work provide the basis for further comparison between lipid biomarkers and other proxies of phytoplankton community structure in the NEECS-WTS.

5.2 Mechanisms of phytoplankton biomass variations revealed by lipid biomarkers

In summer, ∑PB correlated positively with DIN and DIP but negatively with salinity, showing high values in Area I (Fig. 3 d; Table 1). Given the large runoff of the Changjiang River in 2012 (4-14% higher than the mean annual runoff of 1950-2010) (Liu et al., 2012), the markedly low salinity (< 31 PSU) and high nutrient concentrations in Area I (Fig. 2; Table S1) suggest that the summer surface water characteristics and biomass were mainly influenced by the CDW. Previous studies have also shown that the low salinity and eutrophic CDW in summer could reach the Cheju Island, as well as the shelf break, due to high discharge and strong southern monsoon wind (Chen et al., 2008; Lie et al., 2003; Zhang et al., 2007), and phytoplankton biomass in the northern ECS near Cheju Island reflected nutrient

contribution from the Changjiang River (Kim et al., 2009). Our lipid biomarker results provide more evidence of the major role of nutrients from the CDW in enhancing summer biomass in the outer shelf region south of Cheju Island.

In autumn, ∑PB showed no significant correlation with hydrological parameters or nutrients in the whole study area (Table 2). The non-significant correlation between salinity and ∑PB in our study is consistent with the results in Shen et al. (2003), which showed a decrease in Changjiang runoff from summer to winter, suggesting that the CDW may not be the main factor causing high biomass in Area I. On the other hand, the ECS in autumn also receives nutrients from the shelf water of the southern YS (Kim et al., 2009; Umezawa et al., 2014) and from the Kuroshio, which influences surface water from the shelf break to the region off the Changjiang Estuary from autumn to winter (Zhao & Guo, 2011). Thus, we analyzed the complex water masses in autumn in our study area to evaluate their potential roles in the spatial variations of biomarkers (Fig. 5). The *T*-*S* diagram shows two distinct clusters of water masses, with the low salinity shelf water stations (St. 11-14) well separated from the high salinity open ocean water stations (Fig. 5; Table 3). The spatial distributions and *T*-*S* features of the shelf water mass and open ocean water mass are consistent with those of the CCW and ECSSW, respectively, in Qi et al. (2014), potentially suggesting different controlling mechanisms on nutrients and biomass of the two water masses. Thus, correlations between ∑PB and temperature (and salinity and nutrients) were analyzed for the open ocean water stations only (Table 2), as data from the four stations in the shelf water limit correlation analysis efficiency.

In the open ocean water in autumn, ∑PB had significantly negative correlations with temperature and Si:DIP, and significantly positive correlations with DIP (Table 2). The spatial distributions of ∑PB and DIP were also similar, showing a clear increasing trend from south to north, while temperature showed a decreasing trend in our study area (Fig. 2). Further, the low-DIP concentrations ($\leq$ 0.1 μmol L^{-1}) in surface waters only occurred at some stations, with low-DIN ($\leq$ 0.5 μmol L^{-1}) and sufficient Si ($>$ 1 μmol L^{-1}) concentrations were observed at all stations in Fig. 6. Thus, results of correlation analysis in conjunction with spatial distributions and concentrations of nutrients suggest the critical role of DIP on ∑PB.

Similarly, Zhang et al. (2016) also observed that phosphate may be an important factor in controlling Chl-*a* concentration in the autumn of 2008 in the ECS. Moreover, high subsurface Chl-*a* concentrations at station 22 are likely caused by the vertical diffusion of nutrients from subsurface water (Fig. 6). Thus, correlations and spatial distributions of biomarkers and nutrients, together with the vertical profiles of Chl-*a*, suggest that nutrients from subsurface water may be the key factor controlling phytoplankton biomass in the open ocean water in the NEECS-WTS in autumn.

In summary, our results show that phytoplankton biomass in the NEECS-WTS is controlled by different drivers, associated with different water masses, in summer and autumn. In summer, high nutrients from the CDW induced high summer biomass in Area I. In autumn, no single driver could be identified for the high biomass in the whole study area, while nutrients from subsurface water is proposed to be the major factor regulating biomass in the open ocean water. This can be further evaluated and validated by multi-parameter sampling at both surface and subsurface layers in future studies in the NEECS-WTS and more expanded regions.

5.3 Mechanisms of phytoplankton community variations revealed by lipid biomarkers

In summer, the concentrations of both brassicasterol and dinosterol correlated positively with nutrients but negatively with salinity, while C_{37} alkenones showed negative correlations with nutrients but positive correlations with salinity (Table 1). Obviously, there were clear differences in the distribution patterns of the three lipid biomarkers (Fig. 3a-c), indicating niche differentiation of diatoms, dinoflagellates and haptophytes. This result is consistent with the prediction of Margalef (1978), showing that diatoms and dinoflagellates are favored under eutrophic conditions, and haptophytes are more adapted to oligotrophic environments (Baumann et al., 2005; Kinkel et al., 2000; Winder & Sommer, 2012). Our results thus suggest that nutrients derived from the CDW play a major role on phytoplankton community structure in summer, with the different distribution patterns of C_{37} alkenones associated with the different response of haptophytes to the CDW, which did not increase growth of haptophytes but favored the growth of diatoms and dinoflagellates.

In autumn, in the whole study area the three individual lipid biomarkers showed no significant correlation with nutrients or salinity (Table 2). This result is broadly consistent with the findings in Guo et al. (2014), who suggested that more than one factor (high nutrients and turbidity) may regulate phytoplankton community in autumn in the ECS. In the open ocean water stations, we observed that all the three biomarkers correlated negatively with temperature and Si:DIP, and positively with DIP (Table 2), with the three lipid biomarkers and DIP showing a similar distribution pattern (Fig. 2i; Fig. 3f-h). In general, diatoms are favored in high concentrations of inorganic phosphorus at low temperature, high turbulence and low levels of zooplankton grazing; while dinoflagellates and haptophytes are better adapted to the low inorganic phosphorus in a stable water column with increased grazing (Lin et al., 2016; Margalef 1978). Thus, differences in phosphorus acquisition, phosphorus utilization and growth strategies may be a driver of species succession between diatoms, dinoflagellates, haptophytes and other phytoplankton groups (Lin et al., 2016). Our results are consistent with the theoretical basis of phytoplankton community above, showing the dominance of diatoms in the high-DIP Area II and suggesting that DIP associated with water mass (temperature) is more likely the major driver of phytoplankton community structure in the open ocean water in autumn.

6. Conclusions

Spatiotemporal distributions of phytoplankton lipid biomarkers were studied in the NEECS-WTS (including both shelf and open ocean environments) in summer and autumn, with high concentrations of the three lipid biomarkers observed in summer, e.g., up to four to five times higher than those in autumn for mean values of brassicasterol and dinosterol concentrations. For brassicasterol and dinosterol, high-value areas in summer occurred in the southwest of Cheju Island in Area I, while those in autumn were in the south of Cheju Island and the western TS in Areas I and II. For C_{37} alkenones, high-value areas in summer occurred east of Area I and those in autumn were in the south of Cheju Island and the western TS. Similar distributions and positive correlations between ∑PB and Chl-*a* further support the use of lipid biomarker as proxies for assessing phytoplankton biomass in both shelf sea and open

ocean environments. High concentrations of brassicasterol and dinosterol in Areas I and II are consistent with the high abundance of diatoms and dinoflagellates revealed by genes or microscopic data in previous work, validating the use of lipid biomarkers to assess phytoplankton community structure in the NEECS-WTS.

Our results provide one of the first demonstrations of water-mass control on the variations of phytoplankton in the NEECS-WTS as revealed by lipid biomarkers. In summer, nutrients derived from the CDW water mass are the major driver of phytoplankton biomass, with markedly higher nutrient concentrations and biomass in the south of Cheju Island. In autumn, a single driver could not be identified for the high biomass in the whole study area. However, in the open ocean water high subsurface Chl-*a* concentrations at one station in the WTS, along with positive correlations between DIP and ∑PB, suggest that nutrients from subsurface water may stimulate high biomass in the WTS in autumn. Future studies with more spatial coverage, ideally for four seasons' sampling at both surface and subsurface layers of both shelf and open ocean stations, would help to better constrain the mechanisms of phytoplankton biomass and community structure variations for the NEECS-WTS.

Acknowledgments.

We thank Li Li for technical support. We also thank the captains and all of the crew members and scientists on cruise KT-12-25 by the R/V Tansei-maru, cruise NN354 by the T/S Nagasaki-Maru, cruise KH-13-4, and 2013 summer cruise of 973 Program for help with the observations and samplings. Huijun He, Shifeng Yang and Zicheng Wang are acknowledged for helping with water mass analysis. This study was supported by the National Natural Science Foundation of China [grant numbers: 41521064, 41506086, 41276071, 41530965], the "111" Project [grant numbers: B13030], and the JSPS KAKENHI Grant numbers: JP26241009 and JP15H05821. This is MCTL contribution 115. There are no any real or perceived financial conflicts of interests for any author. There are no other affiliations for any author that may be perceived as having a conflict of interest with respect to the results of this paper. The raw data supporting the conclusions can be accessed at https://doi.pangaea.de/10.1594/PANGAEA.887664.

References

Aoyama, M., Goto, H., Kamiya, H., Kaneko, I., Kawae, S., Kodama, H., . . . Toriyama, A. (2008). Marine biogeochemical response to a rapid warming in the main stream of the Kuroshio in the western North Pacific. *Fisheries Oceanography, 17*(3), 206-218. doi:10.1111/j.1365-2419.2008.00473.x

Bai, L., & Zhang, J. (2009). Shelf water mass origins and nutrient flux estimation in the East China Sea using low-volume seawater measurement with rare earth element. *Advances in Geosciences, 18*, 169-180.

Baumann, K.-H., Andruleit, H., Böckel, B., Geisen, M., & Kinkel, H. (2005). The significance of extant coccolithophores as indicators of ocean water masses, surface water temperature, and palaeoproductivity: a review. *Paläontologische Zeitschrift, 79*(1), 93-112. doi:10.1007/BF03021756

Bian, C., Jiang, W., & Greatbatch, R. J. (2013). An exploratory model study of sediment transport sources and deposits in the Bohai Sea, Yellow Sea, and East China Sea. *Journal of Geophysical Research: Oceans, 118*(11), 5908-5923. doi:10.1002/2013JC009116

Bianchi, T. S., & Canuel, E. A. (2011). *Chemical Biomarkers in Aquatic Ecosystems*. Princeton, New Jersey: Princeton University Press.

Boopathi, T., Lee, J. B., Youn, S. H., & Ki, J. S. (2015). Temporal and spatial dynamics of phytoplankton diversity in the East China Sea near Jeju Island (Korea): A pyrosequencing-based study. *Biochemical Systematics and Ecology, 63*, 143-152. doi:10.1016/j.bse.2015.10.002

Chen, C., Xue, P., Ding, P., Beardsley, R. C., Xu, Q., Mao, X., . . . Shi, M. (2008). Physical mechanisms for the offshore detachment of the Changjiang Diluted Water in the East China Sea. *Journal of Geophysical Research: Oceans, 113*(C02002C2), 122-125. doi:10.1029/2006JC003994

Chen, C.T. A., Andreev, A., Kim, K. R., & Yamamoto, M. (2004). Roles of continental shelves and marginal seas in the biogeochemical cycles of the North Pacific Ocean. *Journal of Oceanography, 60*(1), 17-44. doi: 10.1023/B:JOCE.0000038316.56018.d4

Chen, C.T. A., & Borges, A. V. (2009). Reconciling opposing views on carbon cycling in the coastal ocean: Continental shelves as sinks and near-shore ecosystems as sources of atmospheric CO_2. *Deep-Sea Research Part II-Topical Studies in Oceanography, 56*(8-10), 578-590. doi: 10.1016/j.dsr2.2009.01.001

Dong, L., Li, L., Wang, H., Hu, J., & Wei, Y. (2012). Phytoplankton distribution in surface water of Western Pacific during winter, 2008: A study of molecular organic geochemistry. *Marine Geology & Quaternary Geology, 32*(1), 51-59. In Chinese with English Abstract

Furuya, K., Hayashi, M., Yabushita, Y., & Ishikawa, A. (2003). Phytoplankton dynamics in the East China Sea in spring and summer as revealed by HPLC-derived pigment signatures. *Deep Sea Research Part II: Topical Studies in Oceanography*, *50*(2), 367-387. doi: 10.1016/S0967-0645(02)00460-5

Furuya, K., Kurita, K., & Odate, T. (1996). Distribution of phytoplankton in the East China Sea in the winter of 1993. *Journal of Oceanography, 52*(3), 323-333. doi: 10.1007/bf02235927

Gong, G. C., Wen, Y. H., Wang, B. W., & Liu, G. J. (2003). Seasonal variation of chlorophyll *a* concentration, primary production and environmental conditions in the subtropical East China Sea. *Deep-Sea Research Part II: Topical Studies in Oceanography, 50*(6-7), 1219-1236. 10.1016/S0967-0645(03)00019-5

Grasshoff, K., Kremling, K., & Ehrhardt, M. (1999). *Methods of Seawater Analysis.* Weinheim, Germany: WILEY-VCH.

Guo, C., Liu, H., Zheng, L., Song, S., Chen, B., & Huang, B. (2014). Seasonal and spatial patterns of picophytoplankton growth, grazing and distribution in the East China Sea. *Biogeosciences, 11*(7), 1847-1862. doi:10.5194/bg-11-1847-2014b

Guo, S., Feng, Y., Wang, L., Dai, M., Liu, Z., Bai, Y., & Sun, J. (2014). Seasonal variation in the phytoplankton community of a continental-shelf sea: the East China Sea. *Marine Ecology Progress Series, 516*, 103-126. doi:10.3354/meps10952

Guo, S., Sun, J., & Wang, M. (2011). Phytoplankton assemblages in PN section of East China Sea in summer. *Marine Sciences*, *35*, 101-107. In Chinese with English Abstract

Hernandez, M. T., Mills, R. A., & Pancost, R. D. (2008). Algal biomarkers in surface waters around the Crozet plateau. *Organic Geochemistry, 39*(8), 1051-1057. doi:10.1016/j.orggeochem.2008.04.015

Jang, P.-G., Shin, H. H., Baek, S. H., Jang, M. C., Lee, T. S., & Shin, K. (2013). Nutrient distribution and effects on phytoplankton assemblages in the western Korea/Tsushima Strait. *New Zealand Journal of Marine and Freshwater Research, 47*(1), 21-37. doi:10.1080/00288330.2012.718284

Jiao, N., Yang, Y., Hong, N., Ma, Y., Harada, S., Koshikawa, H., & Watanabe, M. (2005). Dynamics of autotrophic picoplankton and heterotrophic bacteria in the East China Sea. *Continental Shelf Research, 25*(10), 1265-1279. doi:10.1016/j.csr.2005.01.002

Kang, L.-K., Lu, H.-M., Sung, P.-T., Chan, Y.-F., Lin, Y.-C., Gong, G.-C., Chiang, K.-P. (2016). The summer distribution of coccolithophores and its relationship to water masses in the East China Sea. *Journal of Oceanography, 72*(6), 883-893. doi: 10.1007/s10872-016-0385-x

Kim, D., Choi, S. H., Kim, K. H., Shim, J., Yoo, S., & Kim, C. H. (2009). Spatial and

temporal variations in nutrient and chlorophyll-*a* concentrations in the northern East China Sea surrounding Cheju Island. *Continental Shelf Research, 29*(11-12), 1426-1436. doi:10.1016/j.csr.2009.03.012

Kinkel, H., Baumann, K.-H., & Čepek, M. (2000). Coccolithophores in the equatorial Atlantic Ocean: response to seasonal and Late Quaternary surface water variability. *Marine Micropaleontology, 39*(1), 87-112. doi:10.1016/S0377-8398(00)00016-5

Li, L., Liu, J., He, J., & Wang, H. (2014). Factors affecting the abundance and community structure of the phytoplankton in northern South China Sea in the summer of 2008: a biomarker study. *Chinese Science Bulletin, 59*(10), 981-991. doi:10.1007/s11434-013-0106-4

Lie, H. J., Cho, C. H., Lee, J. H., & Lee, S. (2003). Structure and eastward extension of the Changjiang River plume in the East China Sea. *Journal of Geophysical Research: Oceans, 108*(C3). doi:10.1029/2001jc001194

Lin, S., Litaker, R. W., & Sunda, W. G. (2016). Phosphorus physiological ecology and molecular mechanisms in marine phytoplankton. *Journal of Phycology*, *52*(1), 10-36. 10.1111/jpy.12365

Liu, D., Chen, S., Mei, J., & Yang, B. (2012). *Changjiang Sediment Bulletin 2012*. Wuhan, China: Changjiang Press. In Chinese

Liu, K.-K., Chao, S.-Y., Lee, H.-J., Gong, G.-C., & Teng, Y.-C. (2010). Seasonal variation of primary productivity in the East China Sea: A numerical study based on coupled physical-biogeochemical model. *Deep-Sea Research Part II: Topical Studies in Oceanography, 57*(19-20), 1762-1782. doi:10.1016/j.dsr2.2010.04.003

Liu, K.-K., Kang, C. K., Kobari, T., Liu, H., Rabouille, C., & Fennel, K. (2014). Biogeochemistry and ecosystems of continental margins in the western North Pacific Ocean and their interactions and responses to external forcing - an overview and synthesis. *Biogeosciences, 11*(23), 7061-7075. doi:10.5194/bg-11-7061-2014

Liu, X., Xiao, W. P., Landry, M. R., Chiang, K. P., Wang, L., & Huang, B. Q. (2016). Responses of phytoplankton communities to environmental variability in the East China Sea. *Ecosystems, 19*(5), 832-849. doi:10.1007/s10021-016-9970-5

Margalef, R. (1978). Life-forms of phytoplankton as survival alternatives in an unstable environment. *Oceanol. Acta., 1*(4), 493-509.

Mejanelle, L., Laureillard, J., Fillaux, J., Saliot, A., & Lambert, C. (1995). Winter distribution of algal pigments in small- and large-size particles in the northeastern Atlantic. *Deep Sea Research Part I: Oceanographic Research Papers, 42*(1), 117-133. doi:10.1016/0967-0637(94)00036-r

Qi, J., Yin, B., Zhang, Q., Yang, D., & Xu, Z. (2014). Analysis of seasonal variation of water masses in East China Sea. *Chinese Journal of Oceanology and Limnology*, *32*(4), 958-971.

Doi: 10.1007/s00343-014-3269-1

Ras, J., Claustre, H., & Uitz, J. (2008). Spatial variability of phytoplankton pigment distributions in the Subtropical South Pacific Ocean: comparison between in situ and predicted data. *Biogeosciences, 5*(2), 353-369. doi:10.5194/bg-5-353-2008

Schubert, C. J., Villanueva, J., Calvert, S. E., Cowie, G. L., von Rad, U., Schulz, H., . . . Erlenkeuser, H. (1998). Stable phytoplankton community structure in the Arabian Sea over the past 200,000 years. *Nature, 394*(6693), 563-566. doi:10.1038/29047

Shen, H. T., Mao, Z. C., & Zhu, J. R. (2003). *Saltwater Intrusion in the Changjiang Estuary*. Beijing: China Ocean Press.

Sicre, M. A., Tian, R. C., & Saliot, A. (1994). Distribution of sterols in the suspended particles of the Chang Jiang Estuary and adjacent East China Sea. *Organic Geochemistry, 21*(1), 1-10. doi:10.1016/0146-6380(94)90083-3

State Bureau of Quality and Technical Supervision (2007). *GB/T 12763-2007 Specifications for Oceanographic Survey*. Beijing: Standards Press of China.

Tolosa, I., Miquel, J.-C., Gasser, B., Raimbault, P., Goyet, C., & Claustre, H. (2008). Distribution of lipid biomarkers and carbon isotope fractionation in contrasting trophic environments of the South East Pacific. *Biogeosciences, 5*(3), 949-968. doi:10.5194/bg-5-949-2008

Umezawa, Y., Yamaguchi, A., Ishizaka, J., Hasegawa, T., Yoshimizu, C., Tayasu, I., . . . Yamawaki, N. (2014). Seasonal shifts in the contributions of the Changjiang River and the Kuroshio Current to nitrate dynamics in the continental shelf of the northern East China Sea based on a nitrate dual isotopic composition approach. *Biogeosciences, 11*(4), 1297-1317. doi:10.5194/bg-11-1297-2014

Wang, Y.-L., Wu, C.-R., & Chao, S.-Y. (2016). Warming and weakening trends of the Kuroshio during 1993-2013. *Geophysical Research Letters, 43*(17), 9200-9207. doi:10.1002/2016gl069432

Winder, M., & Sommer, U. (2012). Phytoplankton response to a changing climate. *Hydrobiologia, 698*(1), 5-16. doi:10.1007/s10750-012-1149-2

Wu, P., Bi, R., Duan, S. S., Jin, H. Y., Chen, J. F., Hao, Q., . . . Zhao, M. X. (2016). Spatiotemporal variations of phytoplankton in the East China Sea and the Yellow Sea revealed by lipid biomarkers. *Journal of Geophysical Research: Biogeosciences, 121*(1), 109-125. doi:10.1002/2015jg003167

Xing, L., Zhang, R., Liu, Y., Zhao, X., Liu, S., Shi, X., & Zhao, M. (2011). Biomarker records of phytoplankton productivity and community structure changes in the Japan Sea over the last 166 kyr. *Quaternary Science Reviews, 30*(19–20), 2666-2675. doi:10.1016/j.quascirev.2011.05.021

Xing, L., Zhao, M., Zhang, T., Yu, M., Duan, S., Zhang, R., . . . Feng, X. (2016). Ecosystem responses to anthropogenic and natural forcing over the last 100 years in the coastal areas of the East China Sea. *Holocene, 26*(5), 669-677. doi:10.1177/0959683615618248

Yuan, R. (2015). *The study on the transports of freshwater and suspended sediment from Changjiang River* (Doctoral dissertation). Retrieved from CNKI. (http://www.cnki.net/KCMS/detail/detail.aspx?QueryID=1&CurRec=11&filename=1015339425.nh&dbname=CDFDLAST2015&dbcode=CDFD&pr=&urlid=&yx=&uid=WEEvREcwSlJHSldRa1FhcTdWajFuajBUVTFzQ2lRd25tUHpFQ1RxdFBsRT0=$9A4hF_YAuvQ5obgVAqNKPCYcEjKensW4ggI8Fm4gTkoUKaID8j8gFw!!&v=MTUxMjhGOVhPcXBFYlBJUjhlWDFMdXhZUzdEaDFUM3FUcldNMUZyQ1VSTEtmWnVSdkZ5N2xWcnpMVkYyNkc3Qzc=). Shanghai, China: East China Normal Univeristy.

Zhang, J., Liu, S. M., Ren, J. L., Wu, Y., & Zhang, G. L. (2007). Nutrient gradients from the eutrophic Changjiang (Yangtze River) Estuary to the oligotrophic Kuroshio waters and re-evaluation of budgets for the East China Sea Shelf. *Progress In Oceanography, 74*(4), 449-478. doi:10.1016/j.pocean.2007.04.019

Zhang, Y., Ding, Y., Li, T., Xue, B., & Guo, Y. (2016). Annual variations of chlorophyll *a* and primary productivity in the East China Sea. *Oceanologia et Limnologia Sinica*, 47(1), 261-268. In Chinese with English Abstract

Zhao, L., & Guo, X. (2011). Influence of cross-shelf water transport on nutrients and phytoplankton in the East China Sea: a model study. *Ocean Science, 7*(1), 27-43. doi:10.5194/os-7-27-2011

Zhao, M. X., Eglinton, G., Haslett, S. K., Jordan, R. W., Sarnthein, M., & Zhang, Z. H. (2000). Marine and terrestrial biomarker records for the last 35,000 years at ODP site 658C off NW Africa. *Organic Geochemistry, 31*(9), 919-930. doi:10.1016/s0146-6380(00)00027-9

Zhao, M. X., Mercer, J. L., Eglinton, G., Higginson, M. J., & Huang, C.-Y. (2006). Comparative molecular biomarker assessment of phytoplankton paleoproductivity for the last 160 kyr off Cap Blanc, NW Africa. *Organic Geochemistry, 37*(1), 72-97. doi:0.1016/j.orggeochem.2005.08.022

Zou, E., Guo, B., Tang, Y., Lee, J.-H., Xiong, X., & Zeng, X. (1999). The hydrographic features and mixture and exchange of sea water in the southern Huanghai Sea in autumn. *Acta Oceanologica Sinica, 21*(5), 12-21. In Chinese with English Abstract

Table 1. Spearman's correlation coefficients between lipid biomarkers and temperature (and salinity and nutrients) in summer.

	Temperature	**Salinity**	**DIN**	**DIP**	**Si**	**DIN:DIP**	**DIN:Si**	**Si:DIP**
B	-0.088	-0.743**	0.577**	0.346*	0.258	0.484*	0.541*	-0.168
D	0.111	-0.606**	0.507**	0.457**	0.068	0.391*	0.478*	-0.340*
A	-0.095	0.360*	-0.340*	-0.022	0.021	-0.479*	-0.428*	-0.006
∑PB	0.050	-0.735**	0.640**	0.475**	0.299	0.504*	0.569**	-0.245
B/∑PB	-0.213	-0.543**	0.606**	0.105	0.218	0.407*	0.668**	-0.012
D/∑PB	0.304*	0.420**	-0.585**	-0.120	-0.298	-0.580**	-0.608**	0.002
A/∑PB	-0.012	0.665**	-0.484**	-0.129	-0.053	-0.574**	-0.546*	0.077

B: brassicasterol; D: dinosterol; A: C_{37} alkenones; ∑PB: the sum of the three lipid biomarkers. **Significant correlation at $p < 0.001$; * Significant correlation at $p < 0.05$

Table 2. Spearman's correlation coefficients between lipid biomarkers and temperature (and salinity and nutrients) in the whole study area and the open ocean water stations in autumn.

	Temperature	Salinity	DIN	DIP	Si	DIN:DIP	DIN:Si	Si:DIP
The whole study area in autumn								
B	-0.482	-0.089	0.075	0.490	0.204	-0.244	-0.118	-0.666**
D	-0.400	-0.011	-0.032	0.366	0.050	-0.275	-0.125	-0.609*
A	-0.196	0.179	-0.097	0.266	-0.086	-0.451	-0.075	-0.292
∑PB	-0.425	-0.025	-0.029	0.454	0.139	-0.363	-0.200	-0.666**
B/∑PB	-0.400	-0.414	0.323	0.327	0.486	0.213	0.043	-0.222
D/∑PB	0.414	0.350	-0.369	-0.377	-0.446	-0.235	-0.168	0.103
A/∑PB	0.236	0.186	-0.201	-0.187	-0.243	-0.209	-0.025	0.319
The open ocean water stations in autumn								
B	-0.942**	-0.018	0.068	0.739*	0.285	-0.400	-0.042	-0.900**
D	-0.973**	-0.103	0.018	0.646*	0.212	-0.400	-0.067	-0.833**
A	-0.632*	0.103	0.185	0.646*	0.042	-0.317	0.188	-0.683*
∑PB	-0.942**	-0.018	0.068	0.739*	0.285	-0.400	-0.042	-0.900**
B/∑PB	-0.146	0.115	0.055	0.197	0.212	0.033	-0.067	-0.400
D/∑PB	<0.001	-0.248	-0.185	-0.332	-0.030	-0.117	-0.152	0.283
A/∑PB	0.231	-0.152	-0.154	-0.098	-0.200	-0.133	-0.067	0.333

B: brassicasterol; D: dinosterol; A: C_{37} alkenones; ∑PB: the sum of the three lipid biomarkers. **Significant correlation at $p < 0.001$; * Significant correlation at $p < 0.05$

Table 3. Surface water mass features in the NEECS-WTS in autumn, including the ranges (mean value) of temperature (℃), salinity (PSU), nutrient concentrations (μmol L^{-1}), biomarker concentrations (ng L^{-1}) and Chl-*a* concentrations (μg L^{-1}).

Water mass	Temperature	Salinity	DIN	DIP	Si	DIN:DIP	B	D	A	∑PB	Chl-*a*	Reference
The Shelf water	22.0-22.8 (22.3)	30.2-30.8 (30.6)	0.2-4.3 (1.5)	0.1-0.4 (0.2)	3.3-16.0 (7.3)	2.8-10.6 (7.6)	40.4-106.1 (62.1)	4.3-14.7 (8.3)	1.4-5.3 (2.9)	50.0-123.8 (73.3)	1.6-3.0 (2.3)	This study
The open ocean water[a]	24.3-27.8 (26.1)	33.3-34.3 (33.7)	0.02-0.5 (0.2)	0-0.1 (0.05)	1.1-3.4 (2.0)	0.3-26 (7.2)	12.1-101.7 (46.9)	2.4-20.5 (8.7)	0.7-7.0 (3.5)	15.2-126.4 (59.0)	0.2-1.1 (0.6)	This study
The CCW	22.0-28.0	27.0-31.0										Qi et al. (2014)
The ECSSW	23.0-28.5	33.0-34.0										Qi et al. (2014)

B: brassicasterol; D: dinosterol; A: C_{37} alkenones; ∑PB: the sum of the three lipid biomarkers. [a] The open ocean water stations include stations 1, 2, 3, 7, 17, 18, 22, 23 and 24. CCW: Continental Coastal Water; ECSSW: East China Sea Surface Water.

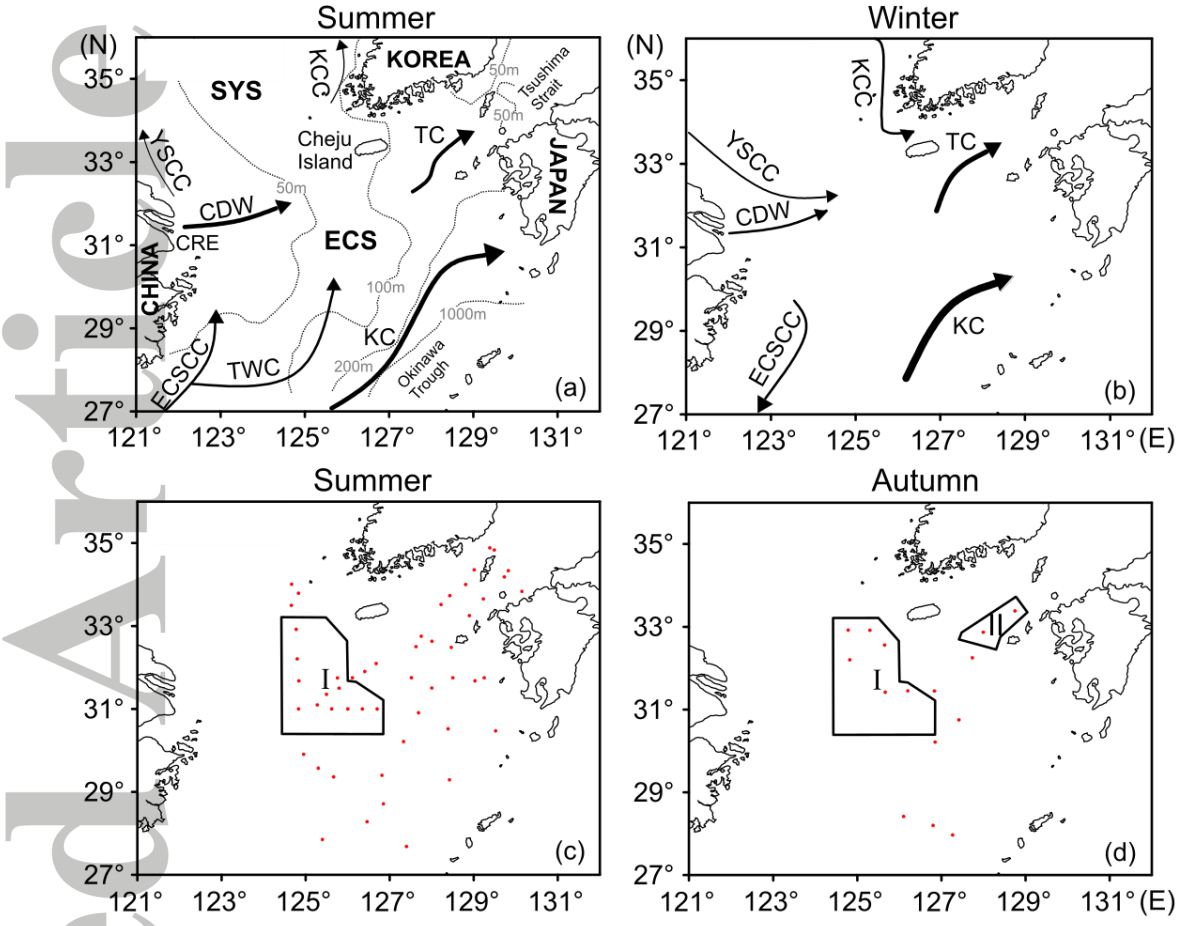

Figure 1. Surface currents in the northeastern East China Sea and the western Tsushima Strait in summer (a) and winter (b), and study areas with sampling stations (red solid dots) and identified high-concentration areas of lipid biomarkers in summer (c) and autumn (d). ECS: East China Sea; SYS: Southern Yellow Sea; CRE: Changjiang River Estuary; KCC: Korea Coastal Current; YSCC: Yellow Sea Coastal Current; CDW: Changjiang Diluted Water; ECSCC: East China Sea Coastal Current; TWC: Taiwan Warm Current; KC: Kuroshio Current; TC: Tsushima Current. Thin solid lines indicate the isobaths. Surface currents in Panels a and b are modified after Bian et al. (2013).

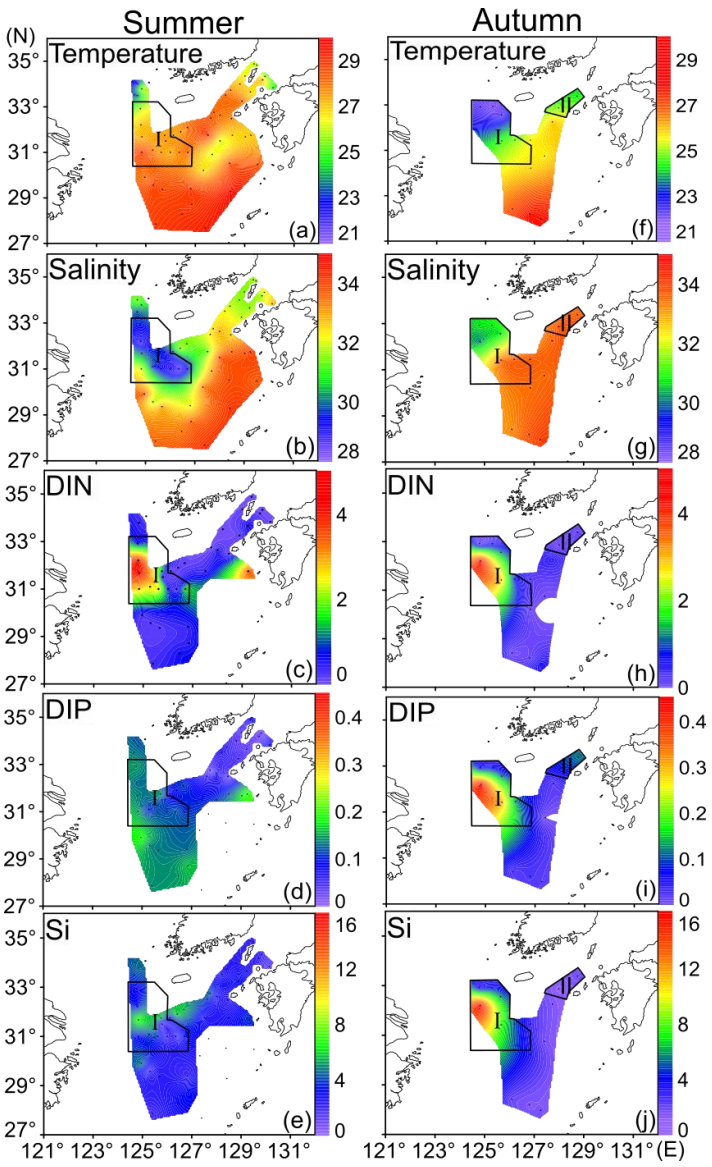

Figure 2. Distributions of temperature (°C; a and f), salinity (PSU; b and g) and nutrients [dissolved inorganic nitrogen (DIN; μmol L^{-1}; c and h); dissolved inorganic phosphorus (DIP; μmol L^{-1}; d and i), and dissolved silicate (Si; μmol L^{-1}; e and j)] in the surface water in the northeastern East China Sea and the western Tsushima Strait in summer (a-e) and autumn (f-j). High-concentration areas of lipid biomarkers are indicated as Area I and Area II. Note that ranges of color bars for each parameter are the same between summer and autumn.

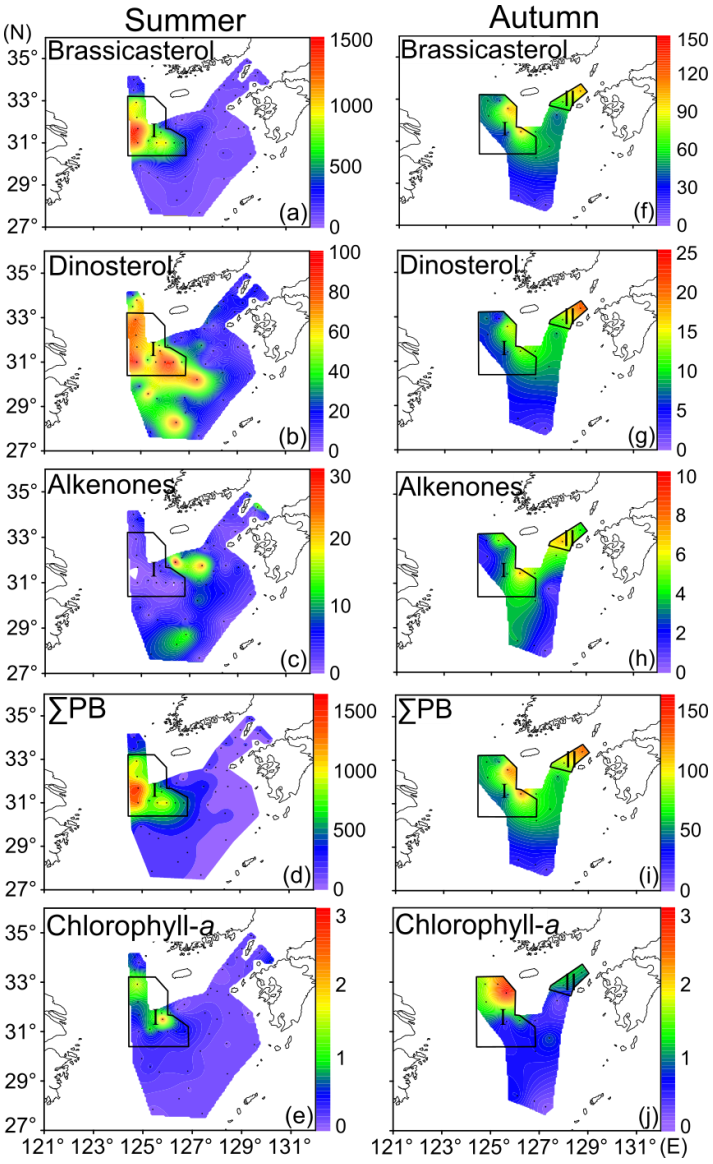

Figure 3. Distributions of lipid biomarkers (ng L^{-1}) and chlorophyll-*a* (μg L^{-1}) in surface suspended particles in the northeastern East China Sea and the western Tsushima Strait in summer (a-e) and autumn (f-j). High-concentration areas of lipid biomarkers are indicated as Area I and Area II. Note that the range of color bar for brassicasterol, dinosterol, alkenones and ∑PB in summer is 10, 4, 3 and 10 times higher than that in autumn, respectively.

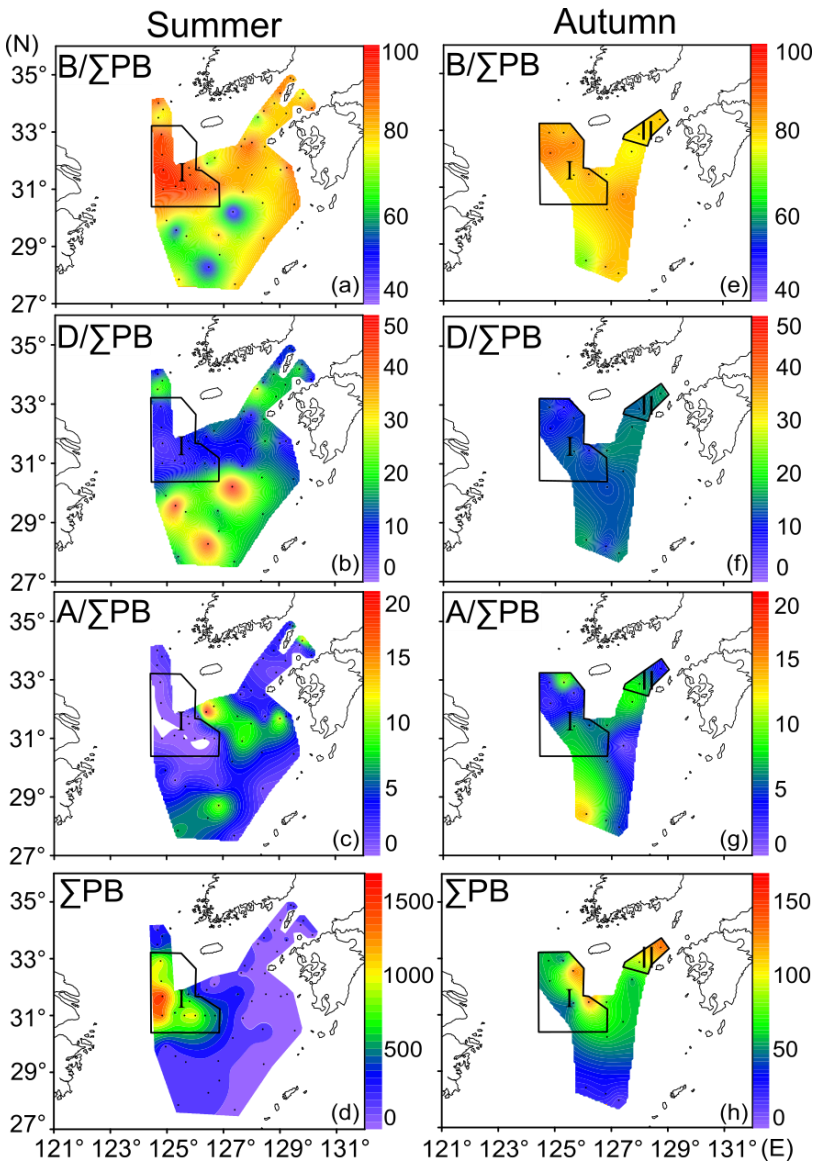

Figure 4. Distributions of individual lipid biomarker proportion [% of ∑PB; B/∑PB (a and e), D/∑PB (b and f) and A/∑PB (c and g)] in surface suspended particles in the northeastern East China Sea and the western Tsushima Strait in summer (a-c) and autumn (e-g). High-concentration areas of lipid biomarkers are indicated as Area I and Area II. Note that ranges of color bar for all parameters are the same between summer and autumn, except for ∑PB where it is 10 times higher in summer than that in autumn.

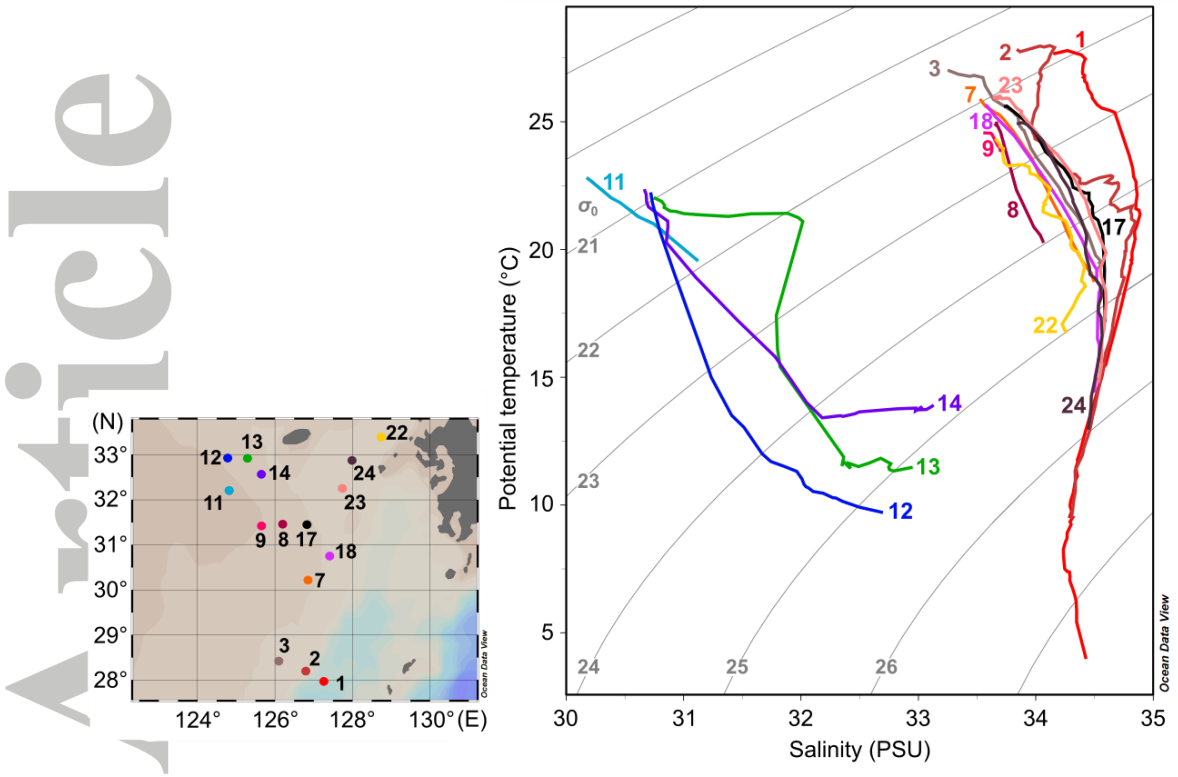

Figure 5. Temperature-salinity diagram in the water column of the northeastern East China Sea and the western Tsushima Strait in the autumn of 2012.

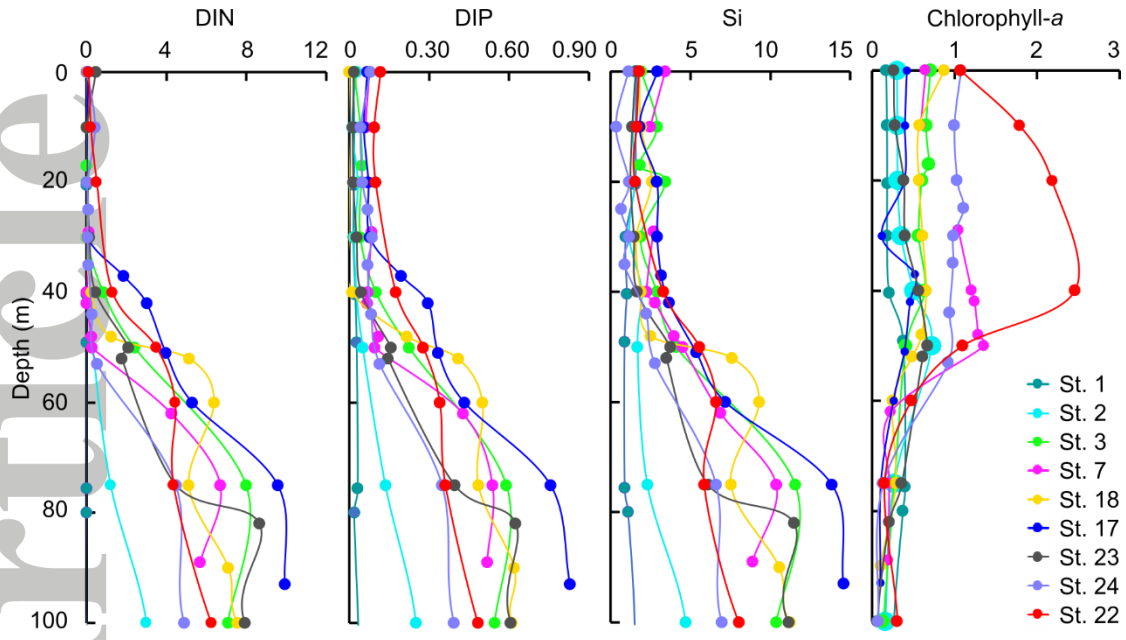

Figure 6. Vertical profiles of dissolved inorganic nitrogen (DIN; μmol L^{-1}), dissolved inorganic phosphorus (DIP; μmol L^{-1}), dissolved silicate (Si; μmol L^{-1}), and chlorophyll-*a* (μg L^{-1}) in the open ocean water stations in autumn of 2012. The location of each station is shown in Fig. 5.